

# Influence of Antibody Immobilization Strategy on Molecular Recognition Force Microscopy Measurements

Kathryn L. Brogan and Mark H. Schoenfish\*

Department of Chemistry, University of North Carolina at Chapel Hill,  
Chapel Hill, North Carolina 27599-3290

Received August 20, 2004. In Final Form: January 14, 2005

A systematic evaluation of the effects of antibody immobilization strategy on the binding efficiency and selectivity (e.g., ability to distinguish between specific and nonspecific interactions) of immunosurfaces prepared with F(ab') antibody fragments of rabbit Immunoglobulin G (IgG) is described. F(ab') was attached to gold surfaces either (1) directly via the formation of a gold-thiolate bond or (2) indirectly through a series of a bifunctional linkers containing an alkane chain or ethylene glycol spacer. Immobilization of F(ab') via the sulfhydryl reactive group located opposite the antigen binding site ensured optimum orientation of the antigen binding site. X-ray photoelectron spectroscopy (XPS) and surface plasmon resonance (SPR) were used to confirm surface modification with the bifunctional linkers and antibody immobilization, respectively. Binding efficiency assays performed with SPR indicated that increasing the length of the linker increased the antigen binding efficiency. Atomic force microscopy (AFM) adhesion force measurements indicated that AFM probes functionalized with directly immobilized F(ab') more effectively discriminated between specific and nonspecific surface-bound proteins than probes modified indirectly via linker-immobilized F(ab'). In addition, a greater number of antibody–antigen binding events were observed with directly immobilized F(ab')-functionalized probes.

## Introduction

Atomic force microscopy (AFM) has been widely used to provide molecular information about specific adhesion forces occurring between biological ligand–receptor pairs.<sup>1–5</sup> Protein-modified tips and substrates have proven useful for investigating highly specific, discrete interactions between biomolecules. The orientation of proteins immobilized on an AFM probe and/or changes in the conformation of surface-adsorbed proteins (i.e., epitope accessibility) may influence the number of binding events and measured interaction forces. Thus, a critical issue in the continued development of molecular-recognition-based AFM involves the immobilization of antibodies onto AFM probes such that they retain biological activity and remain securely attached. Indeed, several antibody immobilization strategies have been pursued to maximize the measurement of antibody–antigen interaction forces.<sup>3,4,6–9</sup>

Antibodies can be immobilized onto AFM probes either directly or indirectly using linker molecules designed to covalently tether the protein to the surface in the proper orientation for maximum antigen binding. Several reports

have focused on the use of tether molecules to immobilize proteins on AFM probes for the measurement of interaction forces.<sup>3,10–14</sup> For example, Dammer and co-workers used ~2.24 nm amine reactive alkane chain spacer arms to attach biotin to bovine serum albumin (BSA).<sup>10</sup> Specific interactions were measured between biotinylated BSA immobilized on an AFM tip and polyclonal biotin-directed Immunoglobulin G (IgG) antibodies immobilized on a substrate. This immobilization strategy purportedly ensured that only specific interactions were measured. Hinterdorfer et al. demonstrated the immobilization of biologically active antibodies on AFM probes via flexible poly(ethylene glycol) (PEG) derivatized thiol linkers ~8 nm in length.<sup>3,4,8,9</sup> The use of such tethers was reported as beneficial for effectively discriminating between specific and nonspecific tip–substrate binding events. PEG linkers have also been used to immobilize proteins for the measurement of ligand–receptor interaction potentials.<sup>11</sup> The addition of a flexible molecular tether was shown to influence the effective reach of the specific ligand–receptor interaction and, therefore, determine the on-rate for the antibody–antigen binding event. Despite the above reports, the utility of antibody immobilization via tethers has been questioned since the flexibility of the linker may allow for multiple antibody orientations during the force measurement experiment.<sup>6,15</sup> Indeed, previous studies have shown that the length of the linker molecule influences the measurement of antibody–antigen inter-

\* To whom correspondence should be addressed. E-mail: schoenfi@email.unc.edu.

(1) Moy, V. T.; Florin, E.-L.; Gaub, H. E. *Colloids Surf., A* **1994**, *93*, 343–348.

(2) Jiang, Y.; Zhu, C.; Ling, L.; Wan, L.; Fang, X.; Bai, C. *Anal. Chem.* **2003**, *75*, 2112–2116.

(3) Hinterdorfer, P.; Baumgartner, W.; Gruber, H. J.; Schilcher, K.; Schindler, H. *Proc. Natl. Acad. Sci. U.S.A.* **1996**, *93*, 3477–3481.

(4) Hinterdorfer, P.; Gruber, H. J.; Kienberger, F.; Kada, G.; Riemer, C.; Borken, C.; Schindler, H. *Colloids Surf., B* **2002**, *23*, 115–123.

(5) Friedsam, C.; Wehle, A. K.; Kuhner, F.; Gaub, H. E. *J. Phys.: Condens. Matter* **2003**, *15*, S1709–S1723.

(6) Willemsen, O. H.; Snel, M. M. E.; van der Werf, K. O.; de Grooth, B. D.; Greve, J.; Hinterdorfer, P.; Gruber, H. J.; Schindler, H.; van Kooyk, Y.; Figdor, C. G. *Biophys. J.* **1998**, *75*, 2220–2228.

(7) Willemsen, O. H.; Snel, M. M. E.; Kuipers, L.; Figdor, C. G.; Greve, J.; de Grooth, B. D. *Biophys. J.* **1999**, *76*, 716–724.

(8) Raab, A.; Han, W.; Badt, D.; Smith-Gill, S. J.; Lindsay, S. M.; Schindler, H.; Hinterdorfer, P. *Nat. Biotechnol.* **1999**, *17*, 902–905.

(9) Hinterdorfer, P.; Schutz, G.; Kienberger, F.; Schindler, H. *Rev. Mol. Biotechnol.* **2001**, *82*, 25–35.

(10) Dammer, U.; Hegner, M.; Anselmetti, D.; Wagner, P.; Dreier, M.; Huber, W.; Guntherodt, H.-J. *Biophys. J.* **1996**, *70*, 2437–2441.

(11) Wong, J. Y.; Kuhl, T. L.; Israelachvili, J. N.; Mullah, N.; Zalipsky, S. *Science* **1997**, *275*, 820–822.

(12) Allen, S.; Chen, X.; Davies, J.; Davies, M. C.; Dawkes, A. C.; Edwards, J. C.; Roberts, C. J.; Sefton, J.; Tendler, S. J. B.; Williams, P. M. *Biochemistry* **1997**, *36*, 7457–7463.

(13) Ros, R.; Schwesinger, F.; Anselmetti, D.; Kubon, M.; Schafer, R.; Pluckthun, A.; Tiefenauer, L. *Proc. Natl. Acad. Sci. U.S.A.* **1998**, *95*, 7402–7405.

(14) Willemsen, O. H.; Cambi, A.; Greve, J.; deGrooth, B. G.; Figdor, C. G. *Biophys. J.* **2000**, *79*, 3267–3281.

(15) Harada, Y.; Kuroda, M.; Ishida, A. *Langmuir* **2000**, *16*, 708–715.

action forces.<sup>6,12</sup> Willemsen and co-workers reported that specific antibody–antigen binding events were observed in only 40% of all force–distance curve measurements for antibody–linker functionalized AFM probes.<sup>6</sup> The 8 nm PEG tether also led to decreased resolution in single molecule imaging experiments due to the larger lateral region of substrate-adsorbed antigen that antibody could interact with.

To avoid the potential limitations of linker immobilization chemistry, Harada and co-workers directly immobilized F(ab) antibody fragments (generated from the enzymatic digestion of IgG with papain) to a gold surface via gold–thiolate bonds between the surface and sulfur groups from the disulfide bridges located in the N-terminal region of the fragment.<sup>15</sup> Direct immobilization ensured that the antibody fragment would be properly oriented on the surface of the AFM tip with the antigen-binding site exposed to solution to increase the probability of antigen binding. In addition, Harada et al. claimed that this approach promoted the enhanced discrimination of specific and nonspecific binding events. The force–distance curves between AFM probes modified with oriented F(ab) antibody fragments and antigen-coated substrates were compared to force curves acquired using gold-coated probes functionalized with a glutaraldehyde cross-linker to randomly immobilize F(ab) in multiple orientations. Differences in the measured antibody–antigen interaction forces were attributed to antibody orientation. Notably, the relative antibody surface coverage for the oriented versus random antibody-immobilization strategies was not examined. Whether the distinction between the different probe-modification strategies was the result of antibody orientation or surface coverage remains unclear.

In the present study, F(ab') fragments that contain a reactive thiol group located at a position structurally opposite the antigen binding site were employed to achieve an oriented antibody immobilization scheme that allowed for a systematic evaluation of the effects of antibody immobilization on the measurement of specific antibody–antigen binding events. Antigen binding of F(ab') IgG fragments directly immobilized to bare gold surfaces via the formation of a gold–thiolate linkage<sup>16</sup> was compared to the antigen binding of antibody fragments which were immobilized using various tethers containing a bifunctional thiol reactive linker coupled to a gold-coated surface. Prior to antibody immobilization, the linker-modified surfaces were characterized by X-ray photoelectron spectroscopy (XPS) and contact angle (surface wettability) measurements. Studies on the influence of the immobilization strategy on antibody surface coverage and subsequent antigen binding efficiency were performed using surface plasmon resonance (SPR). Finally, antibody–antigen binding was evaluated as a function of antibody immobilization strategy using AFM adhesion force measurements between antibody-functionalized AFM probes and both specific and nonspecific surface-bound antigens.

## Materials and Methods

**Reagents.** Rabbit anti-ovalbumin IgG (RAO-IgG) was purchased from Rockland Immunochemical (Gilbertsville, PA). Bovine serum albumin (IgG and protease free) was purchased from Jackson ImmunoResearch (West Grove, PA). Albumin, chicken egg (98%), 11-mercaptoundecanoic acid (11-MUA), ethylenediamine, hexanediamine, dodecanediamine, 2,2'-ethylenedioxy-bis-ethylamine, and 4,7,10-trioxo-1,13-tridecanediamine were purchased from Sigma. Glutaraldehyde and ethanolamine hydrochloride were purchased from Fisher Scientific. (Amino-

propyl)trimethoxysilane (APTMS) was purchased from Gelest (Tulleytown, PA). 1-Ethyl-3-(3-dimethylaminopropyl)carbodiimide (EDC), *N*-hydroxysuccinimide (NHS), and *N*-succinimidyl 3-(2-pyridyldithio)propionate (SPDP) were purchased from Pierce (Rockford, IL). The above chemicals were used without further purification. Water was purified using a Milli-Q UV Gradient A10 System (Millipore Corp., Billerica, MA) to a final resistivity of 18.2 MΩ/cm, and a total organic content of <6 ppb. Other reagents were of analytical grade and used as received.

**Preparation of F(ab') Antibody Fragments.** Rabbit F(ab')<sub>2</sub> fragments were prepared using an ImmunoPure F(ab')<sub>2</sub> preparation kit (Pierce). Rabbit anti-hen ovalbumin (RAO) IgG, 10 mg/mL in 20 mM sodium acetate, pH 4.5 (Rockland Immunochemical), was digested by incubation with immobilized pepsin for 4 h in a high-speed shaker H<sub>2</sub>O bath at 37 °C. F(ab')<sub>2</sub>, Fc fragments and undigested IgG were recovered from the immobilized pepsin. The crude digest was purified using an immobilized Protein A column. The low molecular weight contaminants were removed by dialyzing column eluate against 0.1 M sodium phosphate, 5 mM EDTA buffer (PB) at pH 6.0 with 50 kDa molecular weight cutoff (MWCO) dialysis tubing. F(ab')<sub>2</sub> fragments were concentrated to ~1.5 mg/mL using a centrifugal concentrator with a nominal molecular weight limit (NMWL) of 30 kDa. The final concentrations were determined via absorbance,  $\epsilon = 1.48 \text{ L cm}^{-1} \text{ g}^{-1}$  at 280 nm.<sup>17</sup> Disulfide bonds in the hinge region of the F(ab')<sub>2</sub> fragments were reduced in 50 mM 2-mercaptoethylamine (PB, pH 6.0) via constant mixing for 90 min at 37 °C.<sup>18</sup> The reaction mixture was transferred to a centrifugal concentrator unit with a NMWL of 5000 Da and spun at 5000 rpm to remove excess reducing agent. Additional PB was added to the concentrator unit to prevent precipitation and adsorption of the protein onto the membrane. After the reducing agent was removed, F(ab') fragments were concentrated to ca. 1 mg/mL. Antibody fragments were characterized as described previously.<sup>16</sup>

**Preparation of Gold-Coated Substrates.** Glass cover slips (10.5 × 50 mm, #1 thickness; Electron Microscopy Sciences, Washington, PA) were cleaned in Piranha solution of a 3:7 mixture (v/v) of H<sub>2</sub>O<sub>2</sub> (30%)/H<sub>2</sub>SO<sub>4</sub> (concentrated) to remove organic contaminants. Care should be taken when using Piranha solution since it is a very strong oxidant and can spontaneously detonate upon contact with organic material. The surfaces were rinsed thoroughly with Milli-Q H<sub>2</sub>O and 2-propanol, and dried under a stream of N<sub>2</sub>. Standard silicon nitride (Si<sub>3</sub>N<sub>4</sub>) contact mode AFM probes (Veeco, Santa Barbara, CA) were UV cleaned for 45 min. The glass cover slips and AFM probes were loaded into an ultrahigh vacuum radio frequency argon plasma sputtering system (Kurt J. Lesker Co., Pittsburgh, PA) and coated first with a 3 nm chromium adhesion layer, followed by a 45 nm layer of gold. Thicknesses were monitored using a quartz-crystal microbalance.

**Modification of Gold Surfaces with Thiol–Diamine Bifunctional Reagents.** Linker modified surfaces were prepared by the processes shown schematically in Figure 1. Self-assembled monolayers (SAMs) of 11-mercaptoundecanoic acid were prepared by immersion of the gold-coated substrates in a 1 mM thiol solution (ethanol) for 24 h. The SAM-modified tips were rinsed successively with ethanol, 10% acetic acid (v/v) in H<sub>2</sub>O, ethanol, and then gently dried under a stream of N<sub>2</sub>. Carboxylic acid terminal groups were activated by incubation of the surfaces in a 1:1 (v/v) mixture of 50 mM *N*-hydroxysuccinimide (NHS) and 200 mM 1-ethyl-3-(3-dimethylaminopropyl)carbodiimide (EDC) in H<sub>2</sub>O for 12 h. The substrates were rinsed with H<sub>2</sub>O and dried under a stream of N<sub>2</sub> and then placed in a 10 mM solution of one of the following diamine spacers: ethylenediamine, hexanediamine, 2,2'-ethylenedioxy-bis-ethylamine, or 4,7,10-trioxo-1,13-tridecanediamine in phosphate buffered saline (PBS, pH 7.4) or 10 mM dodecanediamine in ethanol to react for 2 h. The modified surfaces were rinsed with H<sub>2</sub>O and PBS and then placed in a 100 mM solution of ethanolamine pH 8.0 in H<sub>2</sub>O for 1 h to block any remaining unreacted activated sites. Pyridyl disulfide groups were introduced onto the surface by suspending

(16) Brogan, K. L.; Wolfe, K. N.; Jones, P. A.; Schoenfisch, M. H. *Anal. Chim. Acta* **2003**, *496*, 73–80.

(17) Ishikawa, E.; Imagawa, M.; Hashida, S.; Yoshitake, S.; Hamaguchi, Y.; Ueno, T. *J. Immunoassay* **1983**, *4*, 209–327.

(18) O'Brien, J. C.; Jones, V. W.; Porter, M. D.; Mosher, C. L.; Henderson, E. *Anal. Chem.* **2000**, *72*, 703–710.

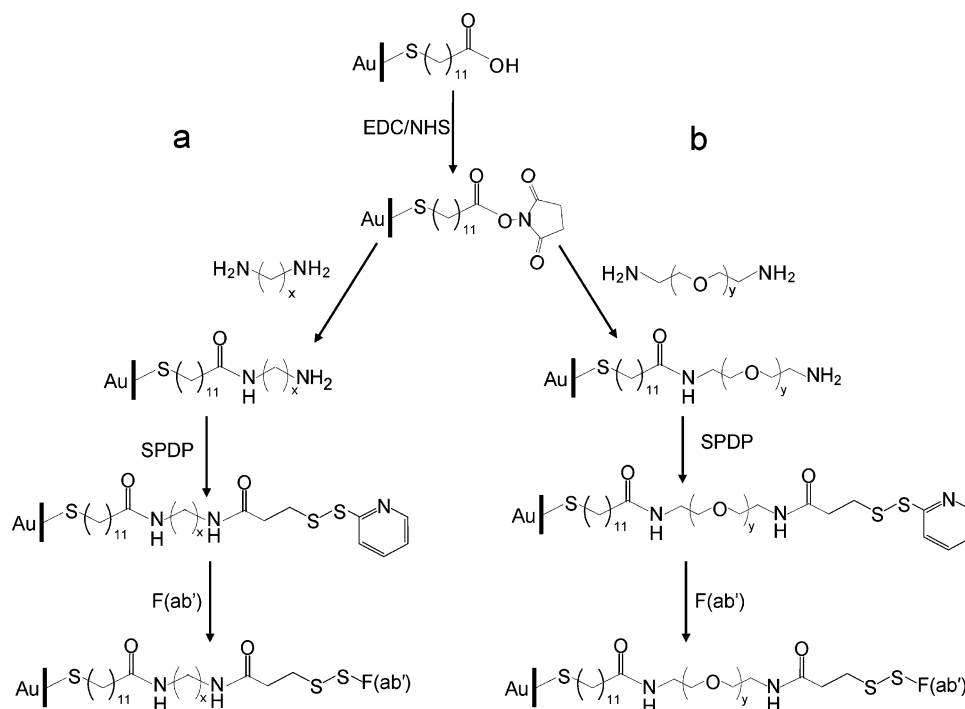


**Figure 1.** Reaction scheme for the preparation of linker modified surfaces with (a) alkane chain diamine molecules (carbon atoms:  $x = 2, 6, 12$ ) and (b) ethylene glycol containing diamine molecules (ethylene glycol units:  $y = 2, 3$ ).

the substrates in a solution of 2 mM *N*-succinimidyl 3-(2-pyridyldithio)propionate (SPDP) in 10% (v/v) dimethyl sulfoxide (DMSO) in PBS, pH 7.4, for 2 h. The surfaces were again rinsed with PBS and stored at 4 °C until further use.

**Preparation of Antibody-Coated AFM Probes.** AFM probes were modified with direct and linker-immobilized antibodies. Directly immobilized antibody surfaces were prepared on freshly sputtered Au-coated tips by reaction for 2 h with rabbit anti-ovalbumin IgG F(ab') fragments (1 mg/mL, phosphate buffer (PB), pH 6.0). The free thiol group of the F(ab') fragment reacts with a gold substrate to form a gold-thiolate bond effectively coupling the antibody to the surface in an oriented manner.<sup>16,18</sup> To evaluate the influence of spacer molecules on force measurements, antibodies were immobilized on sulfhydryl reactive linker-modified gold-coated tips using the procedure described above. The linker-functionalized tips were suspended in rabbit anti-ovalbumin IgG F(ab') fragments (1 mg/mL, PB, pH 6.0) for 2 h at room temperature. The free sulfhydryl on the F(ab') fragment reacts with the terminal pyridyl disulfide covalently attaching the antibody to the surface in an oriented manner, with the antigen binding site exposed to solution.<sup>19</sup>

**Preparation of Protein-Coated Substrates.** Glass slides were silanized by immersion in 10% (v/v) (aminopropyl)trimethoxysilane (APTMS) solution in H<sub>2</sub>O (adjusted to pH 7.0 with acetic acid) for 4 h at 80 °C. Following silanization, the substrates were rinsed with H<sub>2</sub>O and activated by incubation in 10% (v/v) glutaraldehyde solution (H<sub>2</sub>O) for 1 h at room temperature. Surfaces were then modified by incubating in solutions of either hen ovalbumin (HOA, specific antigen) or bovine serum albumin (BSA) (1 mg/mL in PBS) for 1 h. The unreacted glutaraldehyde was blocked via immersion of the surfaces in 100 mM ethanolamine HCl in H<sub>2</sub>O (pH 8.0) for 1 h at room temperature. The protein-coated slides were then rinsed and stored in PBS at 4 °C until further use (no longer than 2 days).

**XPS Characterization of Linker-Modified Surfaces.** XPS measurements were made on linker-modified Au surfaces using a Perkin-Elmer PHI 5400 photoelectron spectrometer equipped with a concentric hemispherical analyzer and a channel electron multiplier detector. The base pressure of the analyzer chamber was ca.  $1 \times 10^{-8}$  Torr. X-rays from the Mg K $\alpha$  line at 1253.6 eV

at a flux of 400 W were used for excitation. Photoelectrons were collected at 45° from the surface normal in the constant analyzer energy (CAE) mode with a pass energy of 35.75 eV. Peak areas were calculated according to the Shirley method.<sup>20</sup> Relative peak area ratios were calculated using previously published photoionization cross sections<sup>21</sup> and accounting for the transmission properties of the analyzer.

**Contact Angle Measurements of Linker-Modified Surfaces.** Static H<sub>2</sub>O contact angle measurements were made on linker-modified Au surfaces using a KSV Instruments CAM 2000 optical contact angle meter (Helsinki, Finland).

**Evaluation of Antigen Binding by Surface Plasmon Resonance.** Antibody surface coverage and antigen binding efficiency were evaluated via SPR using a BIACORE X Biosensor (Pharmacia, Uppsala, Sweden). Sensor chips were prepared in-house following the procedure described above for the preparation of gold-coated surfaces. Freshly sputtered gold chips were used without further modification to evaluate the direct immobilization strategy. Linker surfaces were prepared on gold-modified chips using the procedure detailed above. All further modifications to the surface were carried out in the SPR flow cell with a running buffer of PBS, pH 7.4, containing 0.005% Tween 20. To prepare the immunosurface, a 100  $\mu$ L aliquot of rabbit anti-ovalbumin IgG F(ab') (1 mg/mL) was injected over one channel of the sensor surface at a flow rate of 2  $\mu$ L/min. The second channel was blocked with a 100  $\mu$ L injection of 1 mg/mL bovine serum albumin (BSA, 2  $\mu$ L/min). Loosely associated proteins were removed from the sensor surface by injecting 10  $\mu$ L of 10 mM HCl at a flow rate of 10  $\mu$ L/min. Binding to the immobilized antibody surface was evaluated by a 100  $\mu$ L injection of a 1 mg/mL solution of hen egg ovalbumin (HOA) in PBS, 0.005% (v/v) Tween 20. Refractive index changes were removed by background subtraction of the reference channel. Antigen binding efficiency for each sensor surface was calculated from the equilibrium binding region of the sensorgram.

**Adhesion Force Measurements.** AFM deflection (force) versus distance curves were acquired using a Molecular Imaging Pico Plus SPM (Tempe, AZ) equipped with a liquid cell. The spring constants of the cantilevers were determined independently using a calibration cantilever.<sup>22</sup> Deflection was converted to force using the spring constant of the cantilever. Adhesion

(19) Lu, B.; Xie, J.; Lu, C.; Wu, C.; Wei, Y. *Anal. Chem.* **1995**, *67*, 83–87.

(20) Shirley, D. A. *Phys. Rev. B: Solid State* **1972**, *3*, 4709–4714.

(21) Scofield, J. H. *J. Electron Spectrosc. Relat. Phenom.* **1976**, *8*, 127–137.



**Table 1. X-ray Photoelectron Spectroscopic Data for Linker Modified Surfaces**

surface modification <sup>a</sup>	elemental composition (%)				
	Au	C	N	O	S
11-MUA	20.2	71.8	0.0	6.6	1.3
11-MUA-ED	32.2	54.5	4.0	5.3	4.0
11-MUA-ED-SPDP	30.8	52.9	4.8	7.0	4.5
11-MUA-HD	33.1	50.6	6.0	5.2	5.0
11-MUA-HD-SPDP	29.2	54.8	4.5	6.9	4.6
11-MUA-DD	25.0	64.7	3.9	4.7	1.7
11-MUA-DD-SPDP	12.7	73.9	3.9	7.0	2.5
11-MUA-2,2	27.0	57.7	5.3	6.6	3.5
11-MUA-2,2'-SPDP	28.1	54.4	2.6	10.2	4.6
11-MUA-4,7,10	24.5	59.9	3.8	9.1	2.8
11-MUA-4,7,10-SPDP	27.8	57.7	4.5	6.3	3.8

<sup>a</sup> 11-Mercaptoundecanoic acid (11-MUA), ethylenediamine (ED), hexanediamine (HD), dodecandiamine (DD), 2,2'-ethyleneoxy-bis-ethylamine (2,2'), 4,7,10-trioxa-1,13-tridecanediamine (4,7,10).

forces were calculated using Image Metrology Scanning Probe Image Processor software (Lyngby, Denmark).

## Results and Discussion

Univalent F(ab') antibody fragments were produced from the enzymatic digestion of Immunoglobulin G with pepsin, followed by cleavage of the disulfide bridge in the hinge region of the protein using 2-mercaptoethylamine.<sup>23</sup> As we have previously demonstrated, the free thiol group located opposite the antigen binding site of F(ab') allowed for direct immobilization of the antibody fragment onto a gold surface via formation of a gold–thiolate linkage, ensuring optimum orientation for antigen binding.<sup>16</sup> The thiol group was also used to indirectly immobilize F(ab') to surfaces via thiol-reactive tether molecules, thereby allowing for the evaluation of linker type and length on antigen binding.

**Characterization of Linker-Modified Surfaces.** Linker-modified surfaces were prepared on gold substrates modified with carboxylic acid terminated alkanethiol self-assembled monolayers. The carboxylic acid end groups were converted to *N*-hydroxysuccinimide esters by reaction with EDC and NHS (Figure 1). The resulting activated layer formed amide linkages with diamine spacers yielding an amine-terminated surface, which was then reacted with a bifunctional amine and sulfhydryl-reactive linker to produce the surface used for antibody immobilization. X-ray photoelectron spectroscopy was used to monitor changes in the elemental composition of gold (Au 4f), carbon (C 1s), nitrogen (N 1s), oxygen (O 1s), and sulfur (S 2p) after each reaction step (Table 1). Addition of the alkanethiol self-assembled monolayer of 11-mercaptopundecanoic acid resulted in both an increase in the relative elemental compositions of carbon and oxygen on the surface and the appearance of a peak corresponding to the gold bound thiolate of the SAM in the sulfur region. The relative ratios of nitrogen, oxygen, and sulfur for the ethylenediamine and hexanediamine modified surfaces were slightly lower than the expected 2:1:1 nitrogen to oxygen-to-sulfur ratio. Although the nitrogen-to-sulfur ratio for the dodecanediamine surface was closer to the expected value (2:1), each of the linker-modified surfaces had greater than anticipated amounts of oxygen present which, together with the higher ratios of sulfur, suggested that unreacted carboxylic acid groups were still present on the surface. Incomplete reaction of the carboxylic acid

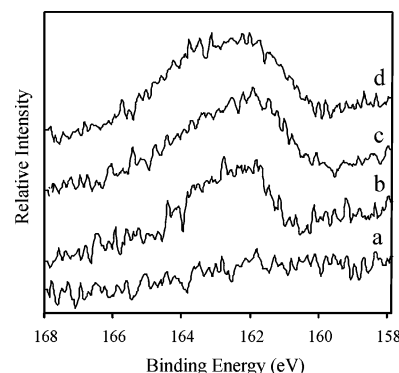


**Figure 2.** XPS spectra for the S 2p binding energy region of (a) bare gold, (b) 11-mercaptopundecanoic acid (11-MUA) SAM on gold, (c) 11-MUA + hexanediamine, and (d) 11-MUA + hexanediamine + *N*-succinimidyl 3-(2-pyridyldithio)propionate (SPDP).

**Table 2. Advancing H<sub>2</sub>O Contact Angles for Linker Modified Surfaces**

surface	$\theta_a$ (deg)
ethylenediamine-SPDP	50.2 ± 2.5
hexanediamine-SPDP	57.1 ± 1.1
dodecanediamine-SPDP	66.0 ± 1.4
2,2'-ethyleneoxy-bis-ethylamine-SPDP	52.3 ± 3.3
4,7,10-trioxa-1,13-tridecanediamine-SPDP	50.4 ± 0.8

groups was somewhat expected based on work by others in this area. Frey et al. reported only 80% conversion efficiency for the reaction of EDC/NHS with a carboxylic acid terminated monolayer, which they attributed to steric packing of the intermediate NHS esters blocking access to some of the 11-MUA carboxylic acid groups, thus preventing complete activation of the surface.<sup>24</sup>

The relative elemental surface compositions for surfaces modified with glycol-containing linkers were close to the expected nitrogen to oxygen to sulfur ratios of 2:3:1 and 2:4:1 for 2,2'-ethyleneoxy-bis-ethylenediamine and 4,7,10-trioxa-1,13-tridecanediamine, respectively. With the addition SPDP, the relative amount of oxygen on each of the surfaces increased indicating covalent attachment of this species. The sulfur regions of the spectra from subsequent modification steps were analyzed to confirm the addition of the terminal disulfide group. An example of the overlaid spectra for the S 2p region of the hexanediamine containing tether is shown in Figure 2. The absence of a peak in the reference spectrum for bare gold (Figure 2a) indicates that the unmodified surface was free of sulfur. Upon the formation of the SAM (Figure 2b), a peak at 162 eV corresponding to the gold-bound thiolate was observed. This peak remained constant with the addition of hexanediamine (Figure 2c). However, after reaction with SPDP, an additional peak at 163.6 eV appeared in the spectrum (Figure 2d). The new peak indicated that the pyridyl disulfide group necessary for F(ab') attachment was successfully bound to the surface and is in agreement with previous reports in which the sulfur peak for a disulfide functional group was shifted to a higher binding energy by ~1 eV.<sup>18</sup> Similar spectra were obtained for the other linkers investigated (data not shown).

The wettability of surfaces used for indirect (tethered) F(ab') immobilization was evaluated using static H<sub>2</sub>O contact angle measurements. Data from the contact angle measurements are shown in Table 2. The variability in the contact angle measurements between the diamine-

(22) Tortonesse, M.; Kirk, M. *SPIE Int. Soc. Opt. Eng.* **1997**, 3009, 53–60.

(23) Nisonoff, A.; Markust, G.; Wissler, F. C. *Nature* **1961**, 4761, 293–295.

(24) Frey, B. L.; Corn, R. M. *Anal. Chem.* **1996**, 68, 3187–3193.

**Table 3. Antibody Fragment Surface Coverage and Antigen Binding Activities Determined by Surface Plasmon Resonance**

linker	RU <sub>F(ab')</sub>	av binding efficiency (%)
F(ab') direct	1458 ± 82	1.9 ± 0.4
ethylenediamine	359 ± 182	14.5 ± 3.7
hexanediamine	827 ± 47	48.7 ± 17.3
dodecanediamine	1107 ± 25	60.9 ± 17.3
2,2'-ethyleneoxy-bis-ethylamine	261 ± 16	25.1 ± 1.8
4,7,10-trioxa-1,13-tridecanediamine	386 ± 41	20.8 ± 3.1

modified substrates indicates nonuniform surface modification. If a closely packed layer were formed, the contact angle values would not be expected to vary as a function of tether length but should instead be governed by the terminal pyridyl group from the SPDP layer. Therefore, the increase in surface hydrophobicity observed as the length of the alkane chain spacer was increased from an ethyl to a dodecyl group suggests exposure of the alkane chains due to nonuniform packing of the diamine linkers. The wettability of surfaces modified with glycol-containing linkers was comparable to that of the ethylenediamine-modified surface. Since similar contact angles values would be expected if the ethylene units of the glycol-containing linkers were exposed, these results suggest that the PEG tethers may not form a closely packed layer on the surface.

**SPR Evaluation of Antibody Immobilization Chemistry.** Surface plasmon resonance was used to evaluate antibody surface coverage and subsequent antigen binding efficiency as a function of antibody immobilization strategy. Antibody orientation has been demonstrated to play a significant role in the antigen binding efficiency of directly immobilized F(ab') immunosurfaces.<sup>16</sup> In the current study, rabbit anti-ovalbumin IgG F(ab') fragments were immobilized either directly onto bare gold SPR sensor chips or indirectly to gold sensor chips modified with the various tether molecules attached to the surface via a carboxylic acid terminated SAM. Antibody surface coverage was determined from the sensor response following antibody immobilization and subsequent rinsing of the surface to remove unbound protein. The antigen binding efficiency of the surface was determined using the following equation

$$\% \text{ binding efficiency} = \frac{\text{RU}_{\text{HOA}} \times \text{MW}_{\text{F(ab')}}}{\text{RU}_{\text{F(ab')}} \times \text{MW}_{\text{HOA}}} \times 100 \quad (1)$$

where RU<sub>HOA</sub> is the sensorgram response upon antigen binding, MW<sub>F(ab')</sub> is the molecular weight of the antibody fragment, RU<sub>F(ab')</sub> is the response due to the initial antibody fragment immobilization, and MW<sub>HOA</sub> is the molecular weight of the antigen. The response due to antibody immobilization and the calculated antigen binding efficiencies are given in Table 3. The surface coverage of bound antibody fragments differed for the various immobilization strategies and tethers employed in this study, with the highest antibody surface coverage corresponding to the direct immobilization of F(ab') onto gold. Notably, the average binding efficiency for this surface was significantly lower than the immunosurfaces prepared via the indirect (linker) immobilization of F(ab'). The low binding efficiency observed for the direct approach (1.9 ± 0.4%) is attributed to a combination of the high packing density of antibody on the surface leading to steric hindrance (thereby reducing access to antigen binding sites) and to the limited antibody motility. Indeed, several reports have demonstrated significant losses in binding activity for surfaces prepared via direct antibody immo-

bilization.<sup>25–28</sup> For example, Vikholm et al. observed reduced antigen binding activity at elevated F(ab') surface coverage for QCM measurements<sup>28,29</sup> and attributed the reduced binding activity to steric blocking of the antigen binding sites in the closely packed antibody layer.

For the indirect (tether-based) immobilization strategies, increases in both the antibody surface coverage and antigen binding efficiency were observed as a function of alkane chain length. Indeed, increasing the tether alkane chain length from ethylenediamine to dodecanediamine led to a 3-fold increase in antibody surface coverage (from 359 ± 182 RU to 1107 ± 25 RU, respectively) and a corresponding enhancement in antigen binding efficiency from 14.5 ± 3.7% to 60.9 ± 17.3%. The significant improvement in the binding efficiencies for the indirectly immobilized F(ab') relative to directly immobilized F(ab') suggests that the motility and flexibility provided by the tether allow the antibody fragment to assume a more appropriate orientation for antigen binding. Of note, large signals were present in the SPR reference channel for antigen binding studies performed with the hexanediamine and dodecanediamine alkane chain linkers, indicating the occurrence of nonspecific interactions between the antigen and the surface immobilized linker. This observation is further supported by the contact angle measurement trends (Table 2) that were attributed to exposure of the alkane subunits. Greater nonspecific adsorption of antigen would be expected at more hydrophobic surfaces.<sup>30</sup> Control experiments with BSA did not show any significant binding to the antibody-coated channel after refractive index changes, and contributions from nonspecific binding to the reference channel (not modified with antibodies) were subtracted from the signal.

Tethers modified with PEG spacers were employed to determine if hydrophobic interactions were occurring between the proteins and the alkane units of the tethers. As shown in Table 3, the antibody surface coverage and antigen binding efficiencies for the PEG linkers (2,2'-ethyleneoxy-bis-ethylamine and 4,7,10-trioxa-1,13-tridecanediamine) were significantly lower than the hexanediamine and dodecanediamine linkers, despite similarities in linker length. Since nonspecific interactions would not be expected to occur between the PEG functional groups and the proteins, it is likely that the values for the alkane linkers are convoluted by the presence of nonspecific interactions. Notably, the binding efficiencies for immunosurfaces prepared with glycol-modified spacers also exhibited greater antigen binding efficiencies than directly immobilized F(ab') surfaces. This further supports the theory that indirect F(ab') immobilization allows for enhanced antibody motility.

Despite higher antigen binding efficiencies, the antibody surface coverage values for the ethylenediamine-modified surface and the two ethylene glycol based linkers were significantly lower than that of the directly immobilized surface. To determine if steric hindrance was a factor in the low binding efficiency observed for directly immobilized F(ab'), the antigen binding efficiency of this immunosurface was evaluated as a function of antibody surface

(25) Alarie, J. P.; Sepaniak, M. J.; Vo-Dinh, T. *Anal. Chim. Acta* **1990**, 229, 169–176.

(26) Spitznagel, T. M.; Jacobs, J. W.; Clark, D. S. *Enzyme Microb. Technol.* **1993**, 15, 916–921.

(27) Vikholm, I.; Albers, W. M.; Valimaki, H.; Helle, H. *Thin Solid Films* **1998**, 327–329, 643–646.

(28) Wimalasena, R. L.; Wilson, G. S. *J. Chromatogr.* **1991**, 572, 85–102.

(29) Vikholm, I.; Albers, W. M. *Langmuir* **1998**, 14, 3865–3872.

(30) Ostuni, E.; Grzybowski, B. A.; Mrksich, M.; Roberts, C. S.; Whitesides, G. M. *Langmuir* **2003**, 19, 1861–1872.

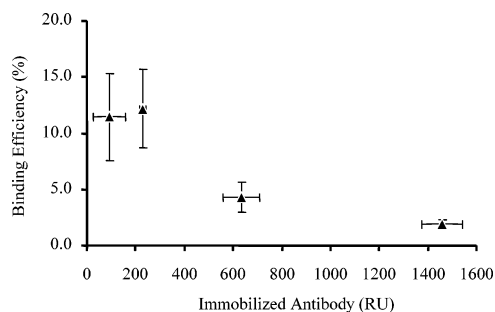


**Figure 3.** Plot of the SPR antigen binding efficiency of directly immobilized F(ab') as a function of antibody fragment surface coverage.

coverage (Figure 3). At low surface concentrations, the calculated binding efficiencies of the immunosurfaces were above 10%. A 3-fold increase in antibody surface coverage from 228 RU to 634 RU corresponded to a 3-fold decrease in the antigen binding efficiency from ~12% to ~4%, respectively. The binding efficiency was further reduced at higher antibody fragment surface coverages. These results indicate that steric hindrance is indeed contributing to the low antigen binding efficiencies observed at high antibody fragment surface concentrations. However, the binding efficiency of directly immobilized antibody fragments, even at low surface coverage levels, was still lower than that of indirectly immobilized F(ab'), suggesting that the additional motility and flexibility may enable the antibody fragment to assume a more ideal orientation for antigen binding in equilibrium-based SPR measurements.

**Adhesion Force Measurements.** To compare the influence of direct and indirect antibody immobilization strategies on the measurement of specific antigen binding events, the adhesion forces between F(ab')-functionalized AFM probes and protein-coated substrates were measured from the attractive region of the unloading portion of a series of force–distance curves. The influence of antibody immobilization strategy on the adhesion forces was evaluated by recording 30 consecutive force curves at 6 different locations on a surface for a minimum of 180 force–distance curves for each tip–substrate combination. Specific antibody–antigen interaction forces were measured on substrates modified with hen ovalbumin (HOA), while surfaces coated with bovine serum albumin (BSA) were used to study nonspecific interactions. The median adhesion force was determined for each tip–sample combination, and a ratio of the specific to nonspecific adhesion force (adhesion force ratio), a measure of the F(ab') modified probe selectivity, was calculated for each immobilization strategy.

Previous work has demonstrated that the time scale for measuring antibody–antigen interactions is critical since the antibody requires adequate time to assume an appropriate conformation for antigen binding.<sup>6,31</sup> Thus, adhesion forces were measured at 125 to 2000 nm/s AFM tip approach/retract rates to determine the optimal loading rate for measuring antibody–antigen binding events between rabbit anti-ovalbumin F(ab')-modified AFM probes and HOA-coated substrates. The specific to nonspecific adhesion force ratios for both direct and indirect F(ab') immobilization as a function of AFM probe loading (i.e., cycling) rate are shown in Figure 4. In general, the specific to nonspecific binding ratio was maximized at a cycling rate of 250 nm/s, regardless of the antibody

immobilization strategy. Indeed, cycling rates greater than 250 nm/s resulted in reduced antigen specificity for each immobilization strategy. The data in subsequent experiments were thus collected at a loading rate of 250 nm/s. Of note, the reduced antigen specificity at faster loading rates was more pronounced for probes modified with linker immobilized F(ab'), which might be expected since the time allowed for a tethered antibody fragment to assume an appropriate orientation for antigen binding would be less at faster cycling rates. Consequently, a potential drawback to using flexible linkers for antibody immobilization for force-related measurements may be the time variability required for the antibody to achieve a proper orientation for antigen binding.

The percentage of force curves characterized by specific and nonspecific binding interactions, the median adhesion force for both specific and nonspecific binding, and the specific to nonspecific adhesion force ratios for the direct and indirect antibody immobilization strategies are quantified in Table 4. Probes functionalized via the direct immobilization of F(ab') fragments were characterized by both the greatest frequency of specific binding and the least nonspecific binding, compared to probes modified with alkane and glycol tethers. As such, AFM probes modified directly with F(ab') were characterized by an enhanced ability to distinguish specific and nonspecific surface-bound antigens over the linker-based methods used in this study. Indeed, the frequency of detected specific adhesion events at HOA-modified substrates decreased for both alkane and glycol linker strategies. Similarly, the number of detected nonspecific adhesion events at BSA-modified substrates increased when linkers were used.

Increasing the length of the alkane antibody tether from ethylenediamine to hexanediamine led to a decrease in both the frequency of measurable interactions (~74 to 41%) and the magnitude of the specific to nonspecific adhesion force ratio (~8.9 to 1.3). This effect is attributed to the hydrophobic nature of the alkane chain, which likely causes the tether to fold and minimize interactions with the surrounding aqueous solution. Consequently, the antibody is more randomly oriented.

Compared to similarly sized alkanethiols, glycol linkers improved the frequency of detected specific interactions from  $41 \pm 11$  and  $30 \pm 9\%$  for hexanediamine and dodecanediamine to  $61 \pm 15$  and  $92 \pm 5$  for 2,2'-ethyleneoxy-bis-ethylamine and 4,7,10-trioxa-1,13-tridecanediamine, respectively. Between the two glycol linkers, the 4,7,10-trioxa-1,13-tridecanediamine was superior when comparing the frequency of detected adhesion events, the median adhesion forces, and the adhesion force ratios. In contrast to the behavior for the alkane linker, this might be expected since a longer tether would enhance antibody fragment mobility because glycol-based linkers are more likely to remain extended, rather than folded in aqueous solution. Improved specificity was also observed with increased tether length ( $1.4 \pm 0.2$  to  $4.0 \pm 2.3$  for 2,2'-ethyleneoxy-bis-ethylamine and 4,7,10-trioxa-1,13-tridecanediamine, respectively), which is attributed to a combination of enhanced F(ab') mobility (enabling appropriate orientation for antigen binding) and lessened nonspecific antigen interactions due to the hydrophilic nature of the glycol subunits.<sup>32</sup> Despite the improvement in the specificity of AFM probes functionalized with F(ab') via glycol tethers, directly immobilized F(ab') still proved superior to the other antibody immobilization strategies investigated in this study.

(31) Lo, Y.-S.; Zhu, Y.-J.; Beebe, T. P. *Langmuir* **2001**, *17*, 3741–3748.

(32) Malmsten, M.; Emoto, K.; Van Alstine, J. M. *J. Colloid Interface Sci.* **1998**, *202*, 507–517.



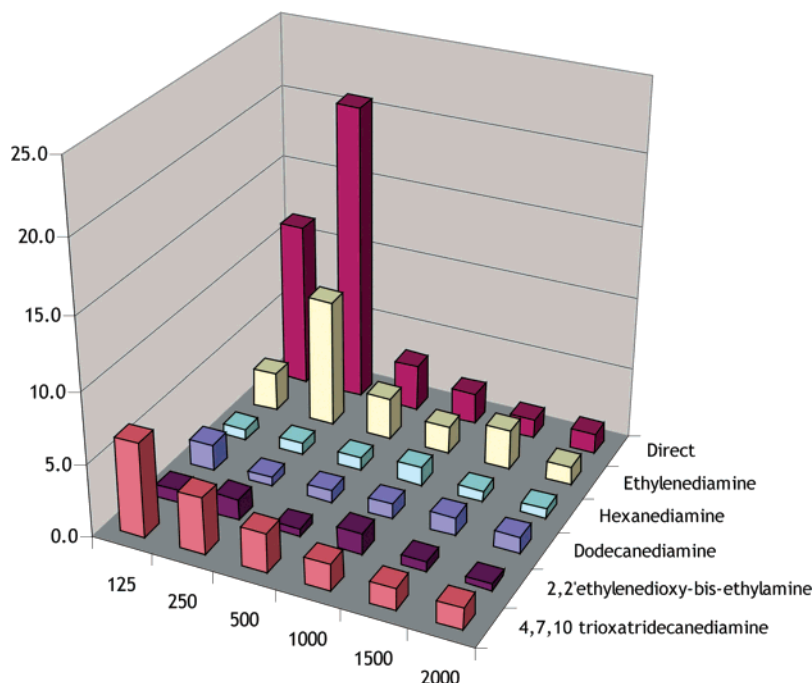


**Figure 4.** Plot of the specific to nonspecific AFM adhesion force ratios at different tip–sample approach rates for the direct and linker-based antibody immobilization strategies.

**Table 4.** Specific to Nonspecific Adhesion Force Ratios for F(ab')-Functionalized AFM Probes Determined at a Cycling Rate of 250 nm/s

immobilization strategy	frequency of detected adhesion events (%) <sup>a</sup>		median adhesion force (nN) <sup>b</sup>		adhesion force ratio <sup>c</sup>
	HOA	BSA	HOA	BSA	
F(ab') direct	95 ± 5	11 ± 7	0.898 ± 0.146	0.044 ± 0.019	20.4 ± 9.4
ethylenediamine	74 ± 26	18 ± 8	0.123 ± 0.590	0.014 ± 0.001	8.9 ± 2.5
hexanediamine	41 ± 11	30 ± 10	0.090 ± 0.045	0.068 ± 0.007	1.3 ± 0.5
dodecanediamine	30 ± 9	17 ± 6	0.046 ± 0.010	0.058 ± 0.004	1.0 ± 0.1
2,2'-ethylenedioxy-bis-ethylamine	61 ± 15	36 ± 11	0.134 ± 0.050	0.093 ± 0.031	1.4 ± 0.2
4,7,10-trioxa-1,13-tridecanediamine	92 ± 5	25 ± 17	0.217 ± 0.043	0.054 ± 0.027	4.0 ± 2.2

<sup>a</sup> Percent of force curves with detectable adhesion events (defined by the presence of a pull-off event as determined from the shape of the force curve.) <sup>b</sup> Error given is the standard deviation of the average of the median adhesion forces. <sup>c</sup> Calculated as the ratio of specific to nonspecific interactions (HOA:BSA).

### Conclusions

Oriented antibody-functionalized surfaces prepared with F(ab') fragments proved useful for evaluating the utility of tethers for measuring antibody–antigen binding interactions. Adhesion force measurements demonstrated that AFM probes functionalized with directly immobilized F(ab') more effectively distinguished between specific and nonspecific surface-bound antigens than probes modified with indirectly immobilized antibody fragments. These studies provide insight into the influence of antibody immobilization strategy on the selectivity of antibody-

functionalized AFM probes and therefore represent an important contribution toward the further development of molecular recognition atomic force microscopy.

**Acknowledgment.** This research was supported in part by the American Chemical Society (PRF 377550-G5), the National Science Foundation (CHE-0349091), and a graduate fellowship from Merck Research Laboratories (K.L.B.).

LA047922Q